Published in AJSE, Vol: 24, Issue:1
Received on 19th January 2025
Revised on 28th March 2025
Published on 31th August 2025

AIUB JOURNAL OF SCIENCE AND ENGINEERING
ISSN: 1608 - 3679 (print) 2520 - 4890 (Online)
https://doi.org/10.53799/xbpw5p60

MHD Convective Casson Ferro-Fluid Flow over Orthogonal Surfaces with Hall Current

Kh. Abdul Maleque, and Kh. Sabikum Malek

***Abstract*— We consider MHD ferro Casson fluid flow across the orthogonal curvilinear surfaces. The unchanged magnetic field parallel to ζ −axis and perpendicular to surfaces, Hall current, heat absorption/generation and nonlinear Casson parameter also examined in our present paper. Pressure gradients and ferro-fluid buoyance forces are dependent on the free stream velocity. The set of governing equations in curvilinear coordinates is changed to a simultaneous dimensionless ordinary differential nonlinear equation by considering suitable nondimensional similarity functions and variable. The missing initial values $[f_{\varphi\varphi}(0), g_{\varphi\varphi}(0), \text{and } \vartheta_{\varphi}(0)]$ have been found from the boundary conditions by shooting method and found the solutions of the dimensionless similarity equations by RK-6 method and construction of numerical program in FORTRAN language. Considering the different values of one parameter and other parameters are kept constant to find the numerical computation. Computational results of numerical solutions were exhibited in figures of momentum and energy by MATLAB and MS Excel. Finally, we have highlighted the comparisons and found a great agreement to justify numerical results acceptable in our study.**

Keywords: Ferro-fluid flow, Nonlinear Casson fluid, Curvilinear surfaces, MHD Flow, Hall current, Heat absorption/generation.

NOMENCLATURES

(ξ, η, ζ) : Curvilinear axes (L),
(U_e, V_e) : Free stream velocity components(L/S),
(h_1, h_2, h_3) : Grabriel lame coefficients,
$T_e = T_0$: Ambient fluid temperature $(°K)$,
β_T:Coefficients of thermal expansion for fluid$(°K)^{-1}$,
μ: Viscosity $(ML^{-1}S^{-1})$,
p: Pressure $(ML^{-1}S^{-2})$,
κ: Thermal conductivity (watt $(meter * °K)^{-1}$),
ϕ: Non dimensional similarity variable,
τ: Shearing stress $(ML^{-1}S^{-2})$,
S_k: Skin friction (dimensionless),
N_u: Non dimensional Nusselt number,
R_e: Non-dimensional Reynold number,
Pr: Non-dimensional Prandtl number,
P_w: Suction/injection parameter (dimensionless),
$(\frac{U_F^2}{U_e^2}, \frac{V_F^2}{V_e^2})$: fluid buoyancy parameters,
m, n, A: exponent constants,
c: dimensionless constant,
ϑ: dimensionless temperature,
(u, v, w): Velocity components in the boundary Layer (LS^{-1}),
$\vec{g} = (g_\xi, g_\eta, 0)$: Gravitational acceleration (LS^{-2}),
T: Temperature inside the boundary layer $(°K)$,
Q_0: Heat generation/absorption ((L^2 $mole^{-1}$),
ρ: Fluid density (ML^{-3}),
ρ_e: Ambient fluid density (ML^{-3}),
C_p: Specific heat with constant pressure,
(f, g): Nondimensional similarity functions,
$\lambda(=\frac{1}{N})$: Casson parameter (dimensionless),
Pr: Dimensionless Prandtl number,
β: Dimensionless heat generation/absorption,
$\vec{B} = (0, 0, B_0)$: Magnetic field (Tesla, Newton/Ampere*meter)
M: Magnetic interaction parameter (dimensionless).
Ω: Hall current (dimensionless),
(a, b): both have dimension (L^{-1})

Kh. Abdul Maleque, Prof. of Mathematics, American International University-Bangladesh. Email: maleque@aiub.edu
Kh. Sabikum Maleque, Student, Dept. of Electrical and Electronics Engineering, American International University-Bangladesh, khsabikum@gmail.com

I. Introduction

THE analysis of boundary layer behavior in fluid mechanics, especially within curvilinear coordinate systems, presents substantial challenges due to the complexities of geometric representation and coordinate transformation. When viscous fluids flow over heated or cooled curvilinear surfaces, distinct velocity and thermal boundary layers are formed and Its influenced by variations in the uniform velocity components and variation of temperature of the surface and fluid of uniform flow. Earlier Hansen [1] studied the classical similarity solution of 3-D boundary layer equations in curvilinear surfaces for focusing solely on forced convection. Later, Zakerullah and Maleque [2], theoretically and numerically investigated incompressible fluid flows in general curvilinear geometries. This work was extended by Maleque [3], who analyzed mixed convective flows over such surfaces. Their analysis included the derivation of similarity requirements and the reformation of the PDEs into simultaneous ODEs. Also, they presented, in tabular form, the possible combinations of free-stream velocity components and temperature gradients. Also, he displayed the various similarity variables in tabular form that change the differential equations of orthogonal curvilinear surface into nondimensional ordinary similarity differential equations.

Further studies on curvilinear coordinate-based fluid flows were conducted by Cebeci et al. [4], Blumberg and Herring [5]. Hung and Brown [6] solved orthogonal Navier Stokes equations by employing finite- difference with implicit method. Redzic [7] investigated the behavior of the vector differential operator ∇ in orthogonal curvilinear coordinates. Flow dynamics within curvilinear channels were analyzed by Mario and Matiaz [8], while Shafiq et al. [9] applied curvilinear coordinates to examine electrically conducting fluid flow over curved surfaces. Derivation of velocity and temperature equations for water accelerated wave surface in curvilinear systems by Kianoosh et al.[10].

For space applications, Barakhoyskaia et al. [11] explored the stabilization of condensate flow over porous curvilinear surfaces. Meneghetti et al. [12] investigated the Navier-Stokes and Poisson equations within curvilinear coordinates using diffeomorphic conformal mapping techniques. More recently, Maleque [13] studied numerical solutions of incompressible fluid and ferrofluid flows over orthogonal curvilinear surfaces, incorporating an effect of heat generation and absorption. These thermal effects have garnered increased attention in industrial applications involving chemical reactions and fluid disintegration processes. Maleque and Sattar [14] analyzed transient magnetohydrodynamic (MHD) convective fluid flow on an infinite rotating disc, including thermal generation and absorption, taking finite difference implicit method (FDIM). Additionally, the results of thermal energy sources with activation energy on unsteady laminar flow over inclined surfaces in chemically reactive fluids were addressed in studies by Maleque [15-16]. The similarity conditions for combined convection boundary layer flows in curvilinear systems were further explored by Maleque [17], contributing to a more comprehensive understanding of fluid transport in complex geometries.

Maleque [18] presented the results of thermal absorption/generation on convective flow in orthogonal permeable surfaces. Heat generative $Al_2O_3 - H_2O$ and $Cu - H_2O$ nanoparticles reaction chemically in one dimensional radiative nanofluid flow investigated by Ramesh [19]. Jalili [20] presented the MHD Jefrey fluid, and chemical reaction across thin object.

Flows of Casson non-Newtonian fluid study garnered considerable to apply one’s mind to the recent decades. Several notable contributions in this area include works by Das [21], Swati [22] and Nadeem [23]. Kaaria and Patel[24] examined Casson MHD fluid flow over the embedded moving permeable surface, accounting for both chemical reactions and thermal radiation.

Maleque [25] explored Casson fluid dynamics under both heating and cooling conditions, incorporating activation energy effects. In another study, Maleque [26] analyzed MHD fluid unsteady flow of Casson fluid in the infinite rotating disc subjected to uniform electric motion. Further extending this line of research, Maleque [27] presented the Hall effect, uniform electric field constant magnetic field over a permeable rotating disc. Also, variable fluid properties and linear thermal radiation are considered in their published paper. More recent studies have expanded on these foundations. Anwar et al. [28] studied time dependent Casson particles flow on vertical thin plate with ramped thermal as well as velocity conditions. Reddy et al. [29] analyzed time-dependent 3-D flow of MHD Casson particle to linearly thin plate perpendicular to the y-axis, considering linear thermal radiation. Lund et al. [30] examined the Joule heating effects on nano Casson fluid on moving thin plate, while Jalili et al. [31] also considered Nano Casson MHD fluid flow over thin plate with linear thermal generation.

Parallel to advancements in Casson fluid dynamics, influence of electric fields and Hall current on the flows has received growing attention due to their relevance applications of engineering such as electromagnetic generators and MHD Hall accelerators. Foundational studies by Pop [32], Gupta [33], and Datta et al. [34] focused on hydromagnetic flows involving Hall current. Ram [35] presented Hall current in free convection concentration flow over permeable object with unchanged magnetic field oriented at an angle to the transverse plane. Sattar [36] analyzed time function MHD natural convective mass transfer flow near permeable sheet, incorporating Hall effect as well as variable suction under constant heat flux.

Hassan and Hazem [37] investigated the Hall effect on steady flow for MHD fluid across the disk. In a related study, Maleque and Sattar [38] analyzed how tangential shear stress at surface of disc induces circumferential as well as radial motion in the flow of fluid due to centrifugal effects. Maleque [39] addressed depth /temperature- -dependent viscosity with Hall effect in time dependent flow over an infinite rotating disc.

Additional contributions included by Uddina and Kumarc [40], who presented Hall current in micropolar flow past a non-conducting wedge. Srinivas Acharya and Shafeeurrahman [41] explored combined convective nanofluid flow with Hall current between concentric cylinders. Prabhakar Reddy [42] analyzed transient MHD flow over a three-dimensional porous rotating plate under Hall effect. More recently, Veera Krishna [42] investigated impacts of radiation, thermo-diffusion and Hall current in micropolar flow across oscillating absorbent sheet. Jitendra Kumar et al. [43] presented transient MHD nanofluid flow with Hall current over the porous channel. Flow study with boundary layer problems of fluid mechanics are so difficult. A uniform fluid flows entering on a motor car, a pipe and an aero foil etc. Our major interest of our problem is to study of velocity and thermal boundary layers across the aerodynamical surfaces. With these in mind, our present paper considered the non-linear Casson parameter and heat absorption/generation on combined forced and natural convective MHD incompressible Casson non-Newtonian fluid flow across vertical curvilinear permeable surfaces. We considered a constant magnetic field $\vec{B} = (0, 0, B_0)$, orthogonal to surface with Hall current effect. Also, Casson parameter $(1+\lambda)^{A}$, where $\lambda = \frac{1}{N}$ has been considered and for nonlinear Casson fluid, $A = \pm 0.5$ has been taken.

We reduced the Prandtl typed governing simultaneous governing PDEs in the orthogonal surfaces into ODEs introducing nondimensional functions and similarity variable. All boundary conditions are changed to initial conditions by shooting method and then the simultaneous ODEs are numerically solved by RK-6 method with numerical program is constructed in FORTRAN LANGUAGE. The results obtained are shown in the figures as momentum per unit mass and temperature distributions. Shearing stress and rate of Thermal flux are displayed in tables with considering different values of various parameters.

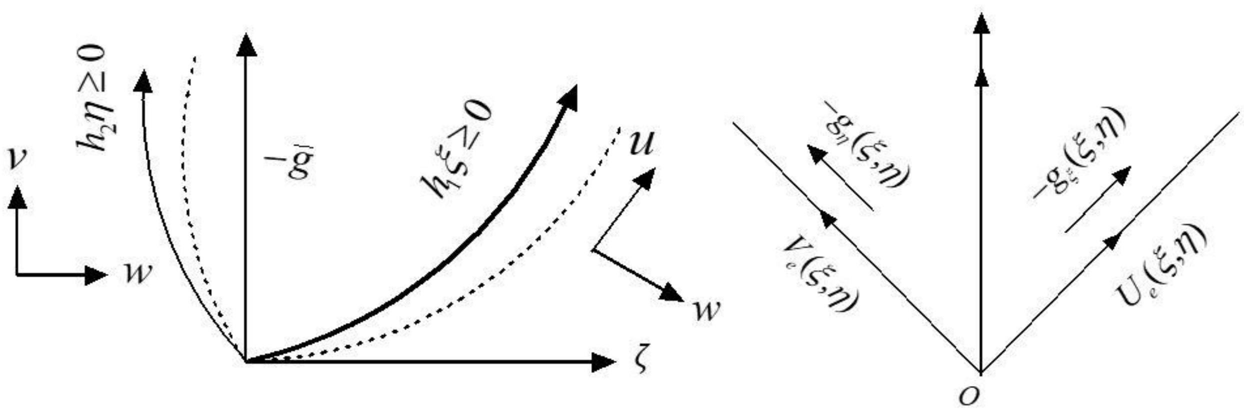

Figure1. Flow configuration in orthogonal surfaces (Maleque [3])

II. PHYSICAL REPRESENTATION AND GOVERNING EQUATIONS

Current density from generalized Ohm's law [Maleque 2009]:

$$\vec{J} = \sigma \left[\vec{E} + \vec{q} \times \vec{B} - \beta_e(\vec{J} \times \vec{B}) \right],$$

The applied constant magnetic field $\vec{B} = (0, 0, B_0)$ orthogonal to the surfaces. Current density components become

$$J_\xi = \frac{\sigma B_0}{1+\Omega^2} (\Omega u + v),$$

and $$J_\eta = \frac{\sigma B_0}{1+\Omega^2} (\Omega \text{v} - u).$$

where, $\Omega = \sigma \beta_e B_0$, the Hall parameter, the Hall factor be $\beta_e = \frac{1}{ne}$; n be unit volume electron concentration; $-e$ be electric charge.

For the present investigation we have considered the heated orthogonal curvilinear inclined vertical surfaces. The outer flow velocity $(U_e, V_e, 0)$ perpendicular to ζ shown in Figure1. For free stream velocity vector $\vec{U}_R = (U_e , V_e , 0)$ and ambient temperature T_e depend on (ξ, η). For the buoyancy force the acceleration vector $\vec{g}(-g_\xi, -g_\eta, 0)$ along $\xi -$ and $\eta -$increasing owing to heated surfaces $(h_1\xi \geq 0,\ h_2\eta \geq 0, \zeta = 0)$. The ferrofluid buoyance forces are $\frac{\sigma_0 M_a}{h_1}\frac{\partial H}{\partial \xi}$ and $\frac{\sigma_0 M_a}{h_2}\frac{\partial H}{\partial \eta}$ considered along $u -$momentum and $v -$momentum respectively. Assuming the pressure gradients and ferrofluid buoyancy forces are dependent on free stream velocity $(U_e, V_e, 0)$. Let the ambient flow conditions $u \to U_e, v \to V_e,\ \rho \to \rho_e,\ T \to T_e(=$ constant), $\frac{\partial}{\partial \zeta} \to 0$ we eliminate the pressure terms $\frac{\partial p}{\partial \xi}$ *and* $\frac{\partial p}{\partial \eta}$ as well as ferrofluid buoyance forces $\frac{\sigma_0 M_a}{h_1}\frac{\partial H}{\partial \xi}$ and $\frac{\sigma_0 M_a}{h_2}\frac{\partial H}{\partial \eta}$, The Prandtl type governing equation as follows (Maleque [3]) in curvilinear coordinates:

Conservation of mass:

$$\frac{\partial}{\partial \xi}(h_2\ u) + \frac{\partial}{\partial \eta}(h_1\ v) + \frac{\partial}{\partial \zeta}(h_1 h_2\ w) = 0, \qquad (1)$$

$u -$momentum:

$$\frac{u}{h_1}\frac{\partial u}{\partial \xi} + \frac{v}{h_2}\frac{\partial u}{\partial \eta} + w\frac{\partial u}{\partial \zeta} + \frac{uv}{h_1 h_2}\frac{\partial h_1}{\partial \eta} - \frac{v^2}{h_1 h_2}\frac{\partial h_2}{\partial \xi} + \frac{V_e^2}{h_1 h_2}\frac{\partial h_2}{\partial \xi} = g_\xi \beta_T (T - T_0) + \left(1 + \frac{1}{N}\right)^A \frac{\partial^2 u}{v \partial \zeta^2} + \frac{U_e}{h_1}\frac{\partial U_e}{\partial \xi} + \frac{V_e}{h_2}\frac{\partial U_e}{\partial \eta} + \frac{U_e V_e}{h_1 h_2}\frac{\partial h_1}{\partial \eta} + \frac{B_0^2 \sigma}{\rho(1+\Omega^2)}[(U_e - u) + \Omega(\text{v} - V_e)] \qquad (2)$$

$v -$momentum:

$$\frac{u}{h_1}\frac{\partial v}{\partial \xi} + \frac{v}{h_2}\frac{\partial v}{\partial \eta} + w\frac{\partial v}{\partial \zeta} + \frac{uv}{h_1 h_2}\frac{\partial h_2}{\partial \xi} - \frac{u^2}{h_1 h_2}\frac{\partial h_1}{\partial \eta} = g_\eta \beta_T (T - T_0) + v\left(1 + \frac{1}{N}\right)^A \frac{\partial^2 v}{\partial \zeta^2} + \frac{U_e}{h_1}\frac{\partial V_e}{\partial \xi} + \frac{V_e}{h_2}\frac{\partial V_e}{\partial \eta} + \frac{U_e V_e}{h_1 h_2}\frac{\partial h_2}{\partial \xi} - \frac{U_e^2}{h_1 h_2}\frac{\partial h_1}{\partial \eta} + \frac{B_0^2 \sigma}{\rho(1+\Omega^2)}[\Omega(U_e - u) + (V_e - v)] \quad (3)$$

Energy:

$$\rho C_p \left(\frac{u}{h_1}\frac{\partial T}{\partial \xi} + \frac{v}{h_2}\frac{\partial T}{\partial \eta} + w\frac{\partial T}{\partial \zeta} \right) = k\frac{\partial^2 T}{\partial \zeta^2} + Q_0 (T - T_0). \qquad (4)$$

Where,

$$-\frac{1}{h_1}\frac{\partial p}{\partial \xi} + \frac{\sigma_0 M_a}{h_1}\frac{\partial H}{\partial \xi} = \rho_e \left(\frac{U_e}{h_1}\frac{\partial U_e}{\partial \xi} + \frac{V_e}{h_2}\frac{\partial U_e}{\partial \eta} + \frac{U_e V_e}{h_1 h_2}\frac{\partial h_1}{\partial \eta} - \frac{V_e^2}{h_1 h_2}\frac{\partial h_2}{\partial \xi} \right) - \frac{B_0^2 \sigma}{1+\Omega^2}(\Omega V_e - U_e) \qquad (5)$$

$$-\frac{1}{h_2}\frac{\partial p}{\partial \eta} + \frac{\sigma_0 M_a}{h_2}\frac{\partial H}{\partial \eta} = \rho_e \left(\frac{U_e}{h_1}\frac{\partial V_e}{\partial \xi} + \frac{V_e}{h_2}\frac{\partial V_e}{\partial \eta} + \frac{U_e V_e}{h_1 h_2}\frac{\partial h_2}{\partial \xi} - \frac{U_e^2}{h_1 h_2}\frac{\partial h_1}{\partial \eta} \right) + \frac{B_0^2 \sigma}{1+\Omega^2}(\Omega U_e + V_e) \qquad (6)$$

$$\rho_e \left(\frac{U_e}{h_1}\frac{\partial T_e}{\partial \xi} + \frac{V_e}{h_2}\frac{\partial T_e}{\partial \eta} \right) = 0. \qquad (7)$$

$T_e = T_0$ (= constant) be the solution of equation (7).

Here, considering $h_3 = 1$, and the original distance ζ calculated that is orthogonal to the surfaces,

The flow field conditions are

$$\left. \begin{array}{l} u = 0, v = 0, w = w_0(\xi, \eta, 0), T = T_w,\ \text{at}\ \zeta = 0. \\ u \to U_e,\ \ v \to V_e,\ T \to T_e\ \ as\ \zeta \to \infty \end{array} \right\} \qquad (8)$$

For the developing surface at $\zeta = 0$ the suction or injection is represented by w_0 for suction velocity $w_0 > 0$ and for injection velocity $w_0 < 0$.

III. SIMILARITY TRANSFORMATIONS

For this paper, following similarity variable and similarity function as well as ambient velocities and temperature are introduced (Maleque [3]) in the Eq1-Eq4:

$U_e = U_0 (a\ \xi + b\ \eta)^m$, $V_e = k_1 U_e$,

$\Delta T = (\Delta T)_0 (a\ \xi + b\ \eta)^{2m-n-1}$, $h_1 = (\xi a + \eta\ b)^n$,

$h_2 = h_1 k_2$, $u = U_e\ f_\phi(\phi),\ v = V_e\ g_\phi(\phi)$,

$T - T_0 = \Delta T \vartheta(\varphi)$, $T_w - T_0 = \Delta T(\xi, \eta)$ and

$$\frac{\varphi}{\zeta} = \left[\frac{(1+m+3n) U_0 a}{2v} \right]^{\frac{1}{2}} (a\xi + b\eta)^{\frac{m-n-1}{2}}.$$

Equations (2-4) take the form:

$$(1+\lambda)^A f_{\varphi\varphi\varphi} + (f+cg)f_{\varphi\varphi} + P_w f_{\varphi\varphi} + \left(\frac{2m}{3n+m+1}\right)\left(1-f_\varphi^2\right)$$
$$+2c\left(\frac{m+n}{3n+m+1}\right)\left(1-f_\varphi g_\varphi\right) - \left(\frac{2nc}{3n+m+1}\right)\left(1-g_\varphi^2\right) + \frac{U_F^2}{U_e^2}\,\vartheta$$
$$+\frac{M}{1+\Omega^2}\left[\left(1-f_\varphi\right) - c\,\Omega\left(1-g_\varphi\right)\right] = 0 \qquad (9)$$

$$(1+\lambda)^A\; g_{\varphi\varphi\varphi} + (f+cg)g_{\varphi\varphi} + P_w g_{\varphi\varphi}$$
$$+\left(\frac{2mc}{3n+m+1}\right)\left(1-g_\varphi^2\right) + 2\left(\frac{m+n}{1+m+3n}\right)\left(1-f_\varphi g_\varphi\right)$$
$$-\left(\frac{2n}{1+m+3n}\right)\left(1-f_\varphi^2\right) + \frac{V_F^2}{V_e^2}\,\vartheta$$
$$+\frac{M}{1+\Omega^2}\left[\Omega\left(1-f_\varphi\right) + c\left(1-g_\varphi\right)\right] = 0 \qquad (10)$$

$$P_r^{-1}\,\vartheta_{\varphi\varphi} + (f+cg)\vartheta_\varphi + P_w\vartheta_\varphi + \beta\,\vartheta$$
$$-2\left(\frac{2m-n-1}{3n+m+1}\right)\left(f_\varphi + c g_\varphi\right)\vartheta = 0. \qquad (11)$$

Where, buoyancy forces of the fluid

$U_F^2 = g_\xi \beta_T\,\Delta T\;\times$ characteristic length

$V_F^2 = g_\eta \beta_T\,\Delta T\;\times$ characteristic length

The characteristic length $= \frac{\xi\,a+\eta\,b}{(1+m+3n)\,a}$.

The dimensionless form of boundary and initial condition (from equation (8)),

$$\left.\begin{array}{l} f(0) = P_w - cg(0),\; f_\varphi(0) = 0, \\ g(0) = g_0,\;\; g_\varphi(0) = 0,\;\; \vartheta(0) = 1, \\ f_\varphi(\infty) = 1, g_\varphi(\infty) = 1,\; \vartheta(\infty) = 0. \end{array}\right\} \qquad (12)$$

Following velocity w is the solution of equation (1) orthogonal to the surface:

$$w = \left(\frac{\nu a U_0}{2}\right)^{\frac{1}{2}} \sqrt{\left(\frac{3n+m+1}{2}\right)}\,(a\,\xi + b\,\eta)^{\frac{m-n-1}{2}}$$
$$\times\left[f + cg - \varphi\left(f_\varphi + c g_\varphi\right)\left(\frac{n-m+1}{m+3n+1}\right)\right] \qquad (13)$$

Where , $P_w = 2w_w\sqrt{\frac{(a\xi+b\eta)^{n+1-m}}{\nu a U_0(3n+m+1)}}$, $\quad c = \frac{k_1 b}{k_2 a}, P_r = \frac{\rho\nu C_p}{k}$,

$\lambda = 1/N, \beta = \frac{Q_0 h_1(a\xi+b\eta)}{a(3n+m+1)\rho C_p U_e}, M = \frac{2h_1(a\xi+b\eta)}{(m+3n+1)}\frac{\sigma B_0^2}{a\,\rho U_e}$.

The conservative condition is $(h_2V_e)_\xi - (h_1U_e)_\eta = 0$, for the outer stream flow we have n= $-m$ otherwise $c = k_1^2$, here n≠ $-m$ is considered.

Using RK-6 method with Nachtsheim-Swigert (1965) iteration scheme the equations (9)-(11) are numerically solved with initial and boundary conditions equation (12). We constructed numerical program in FORTRAN language for the solutions of simultaneous nonlinear ODEs (9)-(11), the numerical results obtained are shown in the figures and in the tables.

IV. PHYSICAL INTEREST

Numerical solutions were calculated for different values of buoyancy parameters $\frac{U_F^2}{U_e^2}$ and $\frac{V_F^2}{V_e^2}$, suction parameter P_w, absorption of heat, Magnetic field, Hall current. Our required physical interest , the numerical results of $f_\phi(0)$, $g_\phi(0)$ and $\varphi(0)$ are shown, therefore, the shear stresses (τ_u, τ_v) and heat flux q_w. Stresses of Shearing $(\tau_u,\ \tau_v)$ and the transfer of heat q_w are found applying the following Newtonian and Fourier formulae :

$$\tau_u = \mu(1+\lambda)^A\left(\frac{\partial\, u}{\partial\zeta} + \frac{1}{h_1}\frac{\partial\, w}{\partial\,\xi}\right)_{\zeta=0},$$

$$\tau_v = \mu(1+\lambda)^A\left(\frac{\partial\, v}{\partial\zeta} + \frac{1}{h_2}\frac{\partial\, w}{\partial\,\eta}\right)_{\zeta=0}, \quad \text{and} \quad q_w = -k\left(\frac{\partial T}{\partial\zeta}\right)_{\zeta=0}.$$

First for u-velocity skin friction

$$S_{ku} = \frac{\tau_u}{\frac{1}{2}\rho\,U_e^2} = (1+\lambda)^A\,R_{eu}^{-\frac{1}{2}}\left[\frac{3n+m+1}{h_1(a\xi+b\eta)}\right]^{\frac{1}{2}} f_{\emptyset\emptyset}(0),$$

Second skin friction for v-velocity

$$S_{kv} = \frac{\tau_v}{\frac{1}{2}\rho\,V_e^2} = (1+\lambda)^A\,R_{ev}^{-\frac{1}{2}}\left[\frac{3n+m+1}{ch_2(a\xi+b\eta)}\right]^{\frac{1}{2}} g_{\emptyset\emptyset}(0),$$

and the Nusselt number

$$N_u = \frac{q_w}{ak\Delta T} = -\,R_{eu}^{\frac{1}{2}}\left[\frac{3n+m+1}{2h_1(a\xi+b\eta)}\right]^{\frac{1}{2}}\;\vartheta_\emptyset(0),$$

where, a and b both have dimension meter^{-1},

$R_{eu} = \frac{U_e}{\upsilon\,a}$, is the primary Reynold number and $R_{ev} = \frac{V_e}{\upsilon\,a}$ is the secondary Reynold number. Noted that $\sqrt{\frac{m+3n+1}{h_1(a\xi+b\eta)}}$ and $\sqrt{\frac{m+3n+1}{ch_2(a\xi+b\eta)}}$ both are dimensionless quantities.

V. THE RESULTS AND DISCUSSIONS

We present the solutions as u and v velocities and temperature for the effects of various parameters $\frac{U_F^2}{U_e^2}$, $\frac{V_F^2}{V_e^2}$, P_w, P_r, m, n, M, Ω *and* c. Numerical results are obtained for one parameter and others are taken as constants. Magnetic interaction parameter(M) and Hall current (Ω) do not enter in temperature equation. Effects of both parameters do not find directly its come through the momentum equations. Magnetic parameter and Hall current effects on temperature profile are not shown.

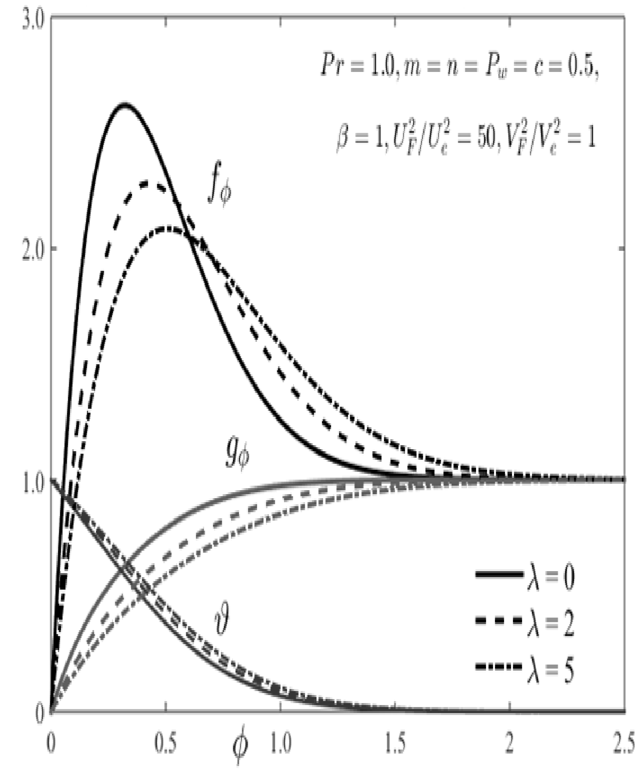

Figure 2. Results of $\lambda\,(=\frac{1}{N})$ on the velocities and temperature distributions for $A = 0.5$

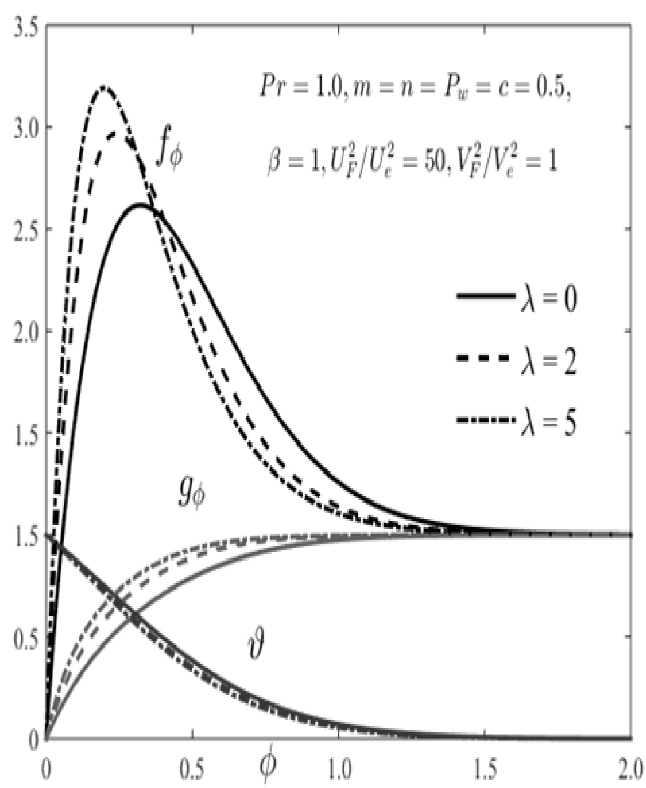

Figure3. Results of $\lambda\,(=\frac{1}{N})$ on the velocities and temperature profiles for $A = -0.5$

A. ***Casson Parameter $\boldsymbol{\lambda}\,(=\frac{1}{N})$ effects:***

In our present paper we consider the nonlinear Casson parameter $\left(1+\frac{1}{N}\right)^{A} = (1+\lambda)^{A}$. Many researchers have considered linear Casson parameter, that is $A = 1$. If $A = 0$ or $\lambda = 0(= N \to \infty)$ indicates Casson fluid is not found that mean Newtonian fluid flow. In this paper we have considered $A = \pm 0.5$ and $\lambda = 0, 2, 5\ (N \to \infty, 0.5, 0.2)$ that is purely nonlinear. The remarkable effects of Casson parameter (λ) are found on $u-$ momentum and $v-$ momentum and the energy profiles are presented in Figures 2-5. In presence of large primary buoyancy force $(\frac{U_F^2}{U_e^2} = 50)$ it has been found from Figure 2 that the primary and secondary both velocities profiles decrease and very small thermal profile increases with λ increases for $A = 0.5$. But from the figure. it is also found that similarity variable $\phi > 0.6$ then the first velocity increase for increasing λ. That is primary boundary layer separations are found at similarity variable ϕ near to 0.6. Opposite effects are found in Figure 3 for $A = -0.5$. For large secondary buoyancy force $(\frac{V_F^2}{V_e^2} = 50)$ it is found from Figure 4 that the primary and secondary both velocities profiles decrease and slightly thermal profile increases with increasing λ for $A = 0.5$. But it has been also found from this figure that similarity variable $\phi > 0.9$ then the $v-$secondary velocity increases in increasing values of λ. That is secondary boundary layer separations are found at similarity variable ϕ near to 0.9. Reverse actions are found for $A = -0.5$ shown in Figure 5.

B. ***Effects of Heat generation and absorption $(\boldsymbol{\beta})$:***

Fig.6 shows thermal generation effect on temperature profile. It is found that the dimensionless heat generation coefficient $(\beta > 0)$ and heat absorption coefficient $(\beta < 0)$ have remarkable effects on temperature, primary velocity and secondary velocity. Assuming $\beta = -1$, represents heat absorption coefficient, and $\beta = 1$ represents generation. $\beta = 0$ shows no effect of the absorption and generation on velocity and temperature. The absorption coefficient has reduced the momentum thickness and temperature thickness are found in Fig6. That is both u-velocity (f_ϕ), v-velocity (g_ϕ)

and T-temperature $(\vartheta_{\emptyset})$ profiles increase with increasing heat generation $(\beta > 0)$ on the other hand, opposite actions are shown in the heat absorption $(\beta < 0)$.

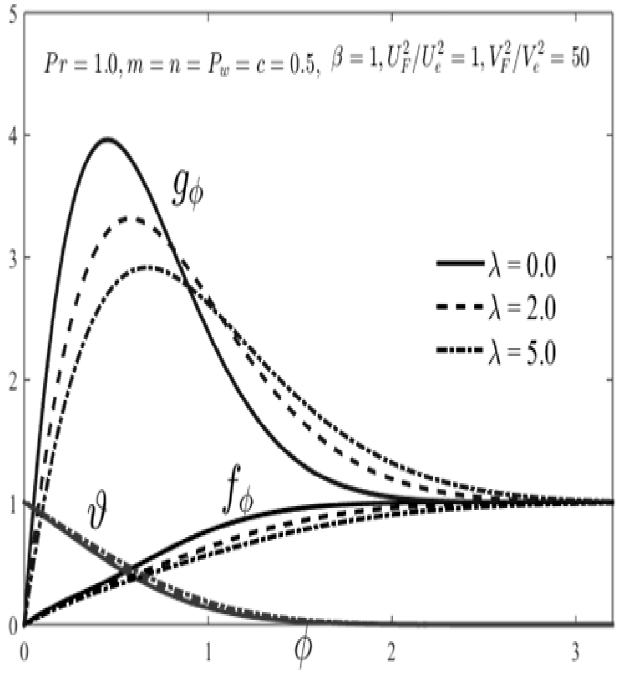

Figure 4. Results of $\lambda\ (= \frac{1}{N})$ on the velocities and temperature profiles for $A = 0.5$

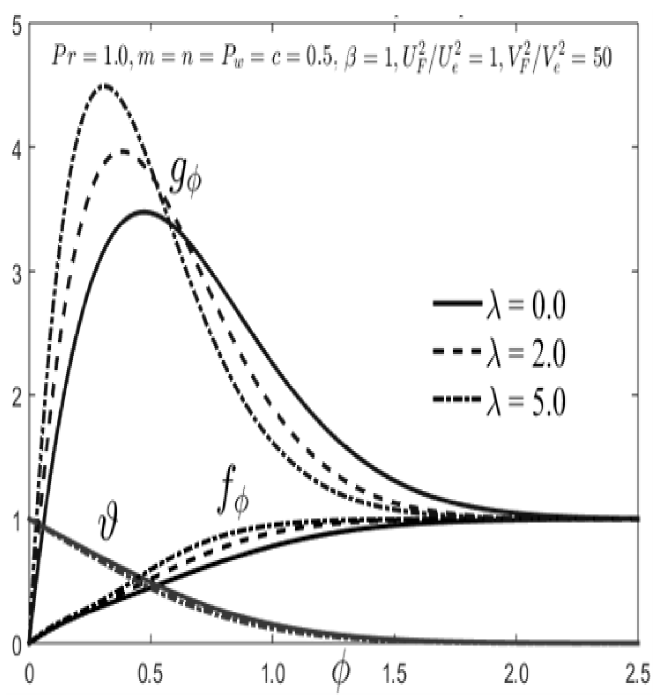

Figure5 Results of $\lambda\ (= \frac{1}{N})$ on the velocities and temperature profiles for $A = -0.5$.

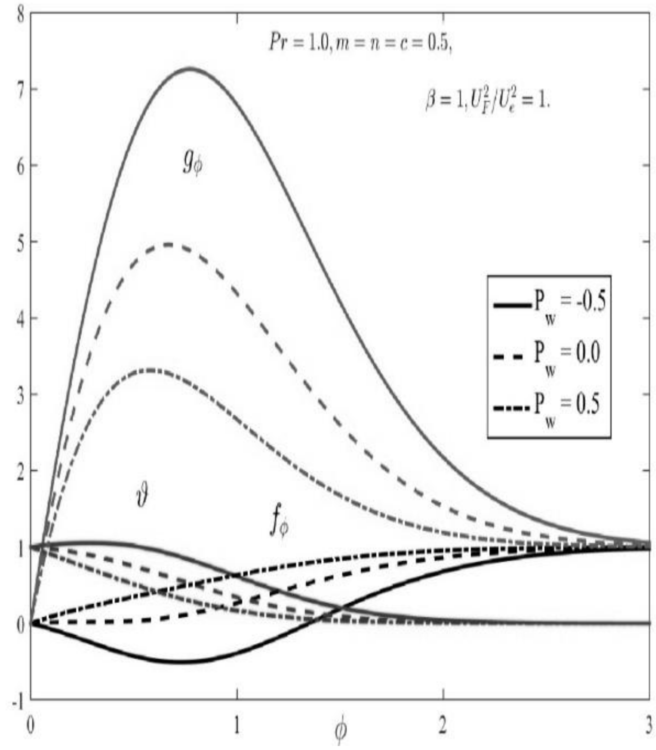

Figure 6. Results of β on velocities and temperature.

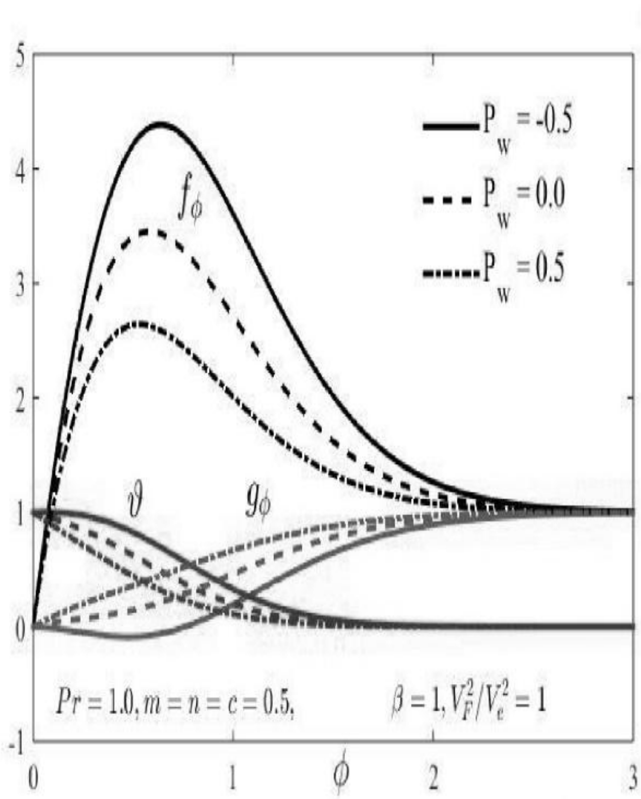

Figure 7. Results of P_w on velocities and temperature for $\frac{U_F^2}{U_e^2} = 50$.

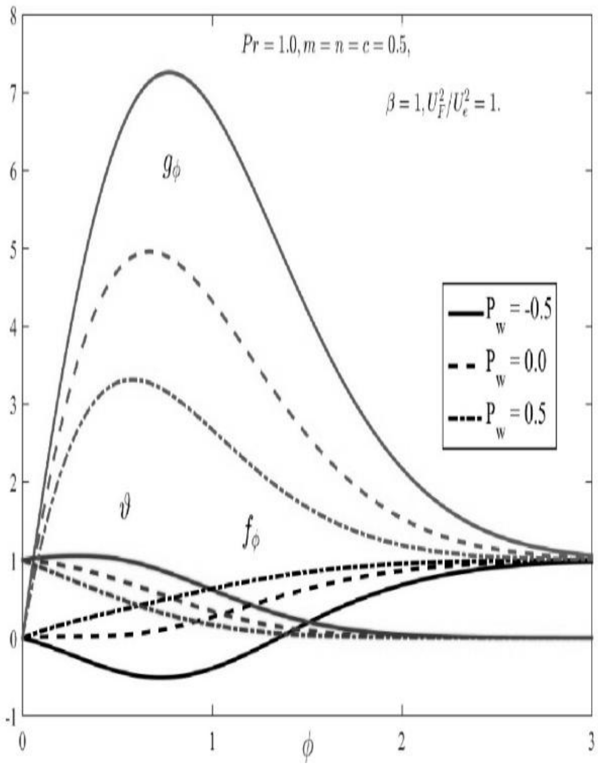

Figure 8. Results of P_w on the velocities and temperature for $\frac{V_F^2}{V_e^2} = 50$.

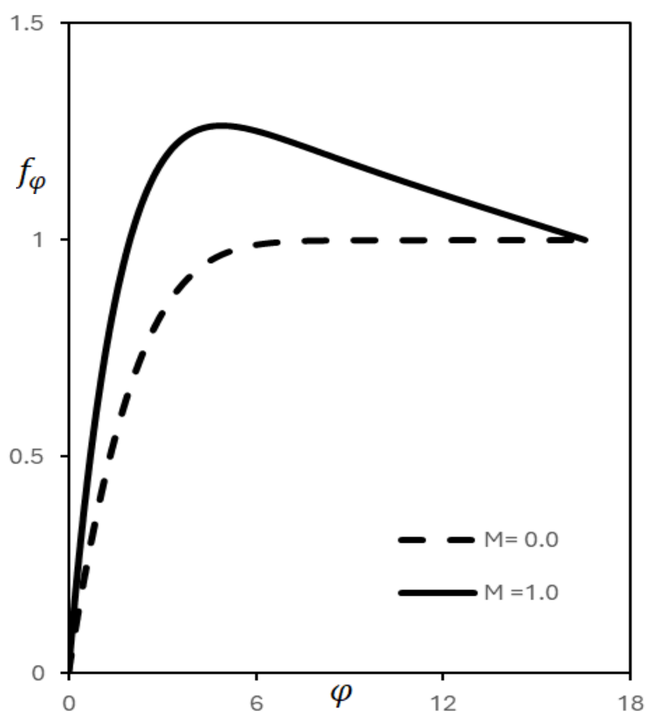

Figure 9. u−velocity profile increases for increasing values of M

The thickness between the surface and ambient temperature increases for increasing heat generation coefficient. From figure 6, It is also found that heat generation leads to increase velocities and temperature. For integrating heat absorption, the momentum and temperature have been overshooting, that indicates the momentum boundary layer and temperature thickness are close to surfaces.

Table-1 shows that the shearing stress and heat flux are significantly changing for thermal generation. Heat absorption effect is to contract the momentum and energy layers. As well as generation is to expand the momentum and energy thickness. Heat flux increases for absorption increases means more temperature needed throughout the surfaces to hold the isothermal surfaces.

C. Suction/injection parameter (P_w) effects:

Figure 7 and Figure 8 show suction and injection parameter P_w effects on u-velocity, v-velocity and temperature. In Figure 7, $P_w = -1, 0, 1$ are considered for fixed values of $\frac{U_F^2}{U_e^2} = 50$ and $\frac{V_F^2}{V_e^2} = 1$. The suction, the injection, the section, and no suction/injection are represented by $P_w > 0$, $P_w < 0$, and $P_w = 0$ respectively.

Figure 7 shows that u- velocity (primary) and temperature decrease for increasing suction parameter P_w and opposite effects are found for v-velocity (secondary) profile. That is, the increasing values of P_w has reduced primary momentum and energy layers for large value of primary buoyancy force $\frac{U_F^2}{U_e^2} = 50$. On the other hand, $P_w = -1, 0, 1$ are assumed for constant values of $\frac{U_F^2}{U_e^2} = 1$ and $\frac{V_F^2}{V_e^2} = 50$ shown in Figure 8. We also found from Fig 8, the reverse actions have come upon in the velocities for large value of $\frac{V_F^2}{V_e^2} = 50$, similar effects come from energy. Accelerating suction Pw conducts to temperature and v- velocity decrease, and u- velocity (primary) increases. The layer thickness of the secondary velocity and the layer of temperature are decreased for the P_w increases for high value of $\frac{V_F^2}{V_e^2} = 50$. Influence of suction parameter P_w on the coefficients of shearing stresses and

Nusselt number coefficient for $c = m = n = Pw = 0.5, Pr = 1.0,\ \frac{U_F^2}{U_e^2} = 10,\ \frac{V_F^2}{V_e^2} = 5$ are shown in table2. This is found that increasing P_w leads skin frictions accelerate, also the heat flux reduces.

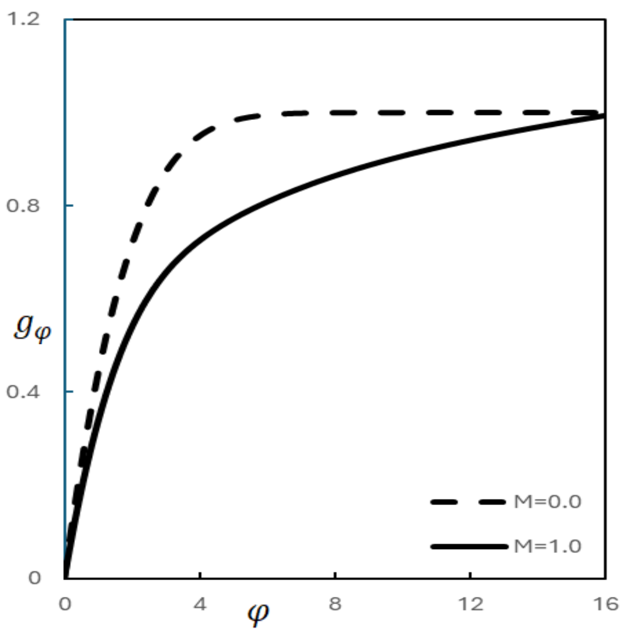

Figure 10. v–velocity profiles decrease for increasing values of M

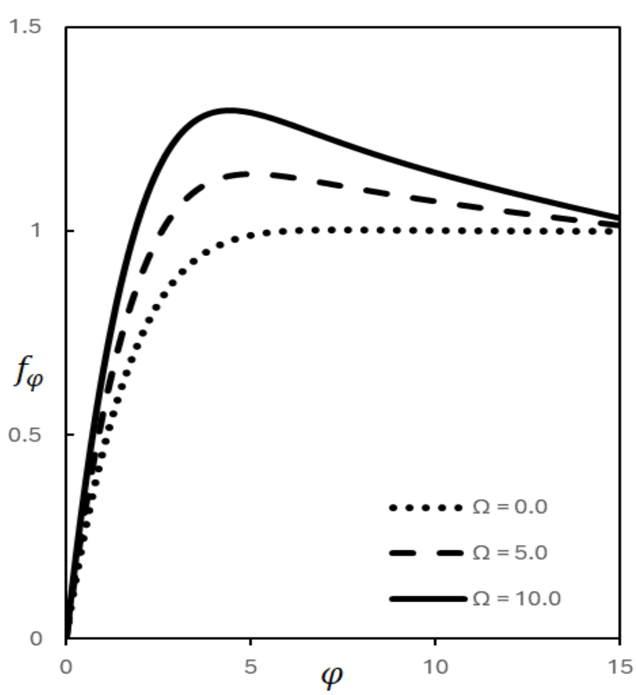

Figure 11. u–velocity profiles increase for increasing values of Hall current Ω

D. ***Magnetic interaction parameter (M) effects:***

The transverse magnetic field acts parallel to ζ −axis and orthogonal to the surfaces. Fig9 and Fig10 respectively show the magnetic force effects on $u-$ momentum and $v-$ momentum. Figures present that $u-$ velocity increases while the $v-$ velocity decreases for increasing value of nondimensional magnetic interaction M. Because of that from equation14, $\frac{M}{1+\Omega^2}(1-f_\varphi)$ represents $f_\phi \propto (1-\frac{()}{M})$ that means for fixed value of Hall current $\Omega = 0.5$, it has been found f_ϕ increases for increasing values M shown in Fig.9. Again, from equation 14, $\frac{M}{1+\Omega^2}[\Omega c(g_\varphi - 1)]$ represents $g_\phi \propto (1+\frac{()}{M})$ that means for fixed value of $\Omega = c = 0.5$, g_ϕ decreases for increasing values of M. Physical representation of the result, the magnetic field interacts with the electric current providing rise to Lorentz force along $\zeta -$ direction that resists the fluid motion that is secondary velocity decreases.

E. ***Hall current (Ω) effects:***

Principle of Hall current expresses the charge carrier behavior bears when it is expanded to electricity and magnetic field. The principle also can be regarded as an extension of Lorentz force that is the acting on the charge carriers (Electron and Holes) passing through the magnetic field. Effects of Hall current on the velocities are shown in Figure 11 and 12 respectively. Figures present the momentum(u) accelerates and momentum(v) decelerate with Hall current (Ω) increases. Because of $\Omega = \sigma\beta_e B_0$. Hall current ($\Omega$) plays the same role of M on u −momentum and $v-$ momentum profiles. Although from equation (14), we found that $\frac{M}{1+\Omega^2} f_\phi$ => $f_\phi \propto (1+\Omega^2)$ that is for fixed value of M, Hall current (Ω) leads in increase the primary velocity (f_ϕ) found in Fig.11. Again $\frac{M\,\Omega}{1+\Omega^2} g_\phi$ indicates secondary velocity (g_ϕ) decreases with Hall current (Ω) increases found in Fig.12.

COMPARISON

Assuming $A = 0,\quad \beta = 0,\quad c = 0,\quad M = 0,\quad n = 0,$ $\Omega = 0$ and $P_w = 0$ in the above equations (9), we have found the well-known Falkner-Skan equation (Schlichting [45]). Moreover, if $A = c = M = \Omega = k_1 = U_F = \beta = P_w = 0,$

the equation (9) shows great agreement with Sparrow's [46] equation. It is found the justification of our analytic work. Table-3 shows the comparison between the numerical results of Falkner Skan equation by Vasile et al. [47] and the present work for $\frac{2m}{m+1} = 0.5$, and all other parameters kept zero.

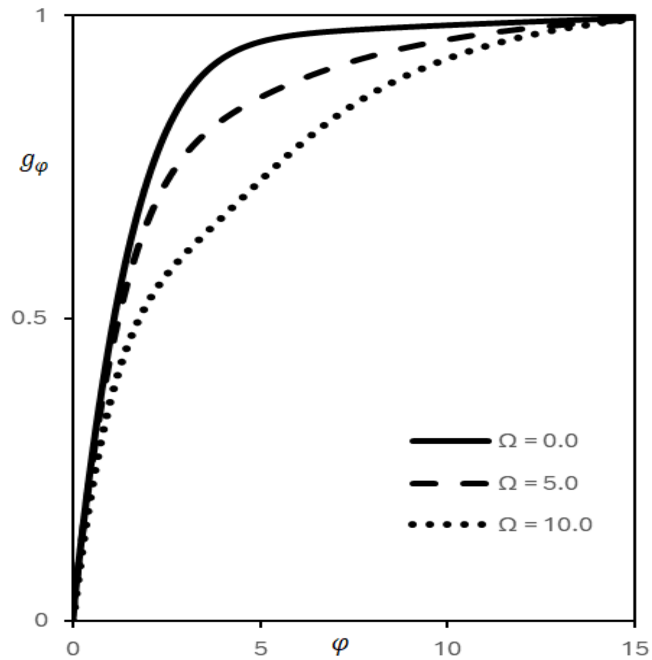

Figure 12. v−velocity profiles decrease for increasing values of Hall current Ω

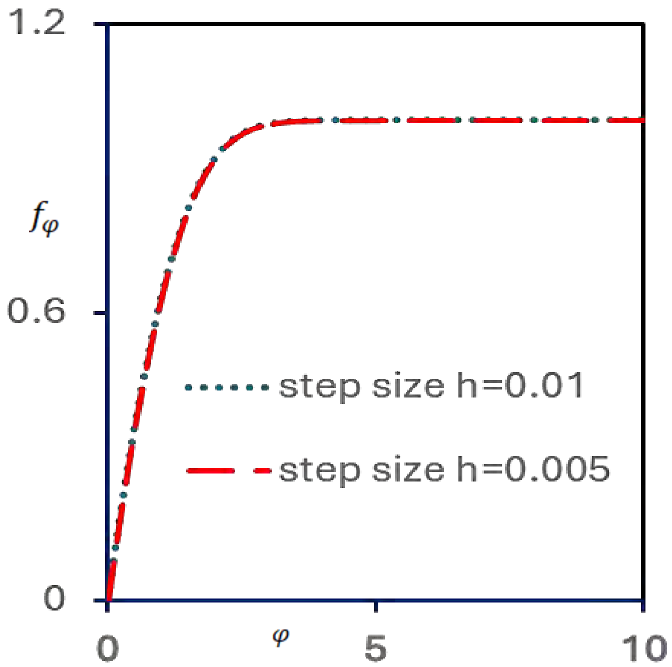

Figure 13. Effect of different step sizes

Table-3 shows the relative error near to zero. That is clearly found that well convergence (agreement) between the present and Vasile Marinca et al. [47] results.

Finally figure 13. Shows the velocity profiles for different values of step sizes h=0.01 and h=0.005. It has been observed from this figure that the validity of numerical solutions. In this case, the step size was assumed be $h = 0.01$ that satisfied with 10^{-6} convergence criteria. Although, variation of step sizes that is $h = 0.01$, and $h = 0.005$ were also considered and the obtained results show that it does not depend on the step sizes found in Figure 13.

VI. CONCLUSIONS

In fluid mechanics, the boundary layer over curvilinear surface is a complicated problem. In the present paper, effects of the non-linear Casson parameter, heat absorption/generation and suction on mixed free and forced convection flow over orthogonal curvilinear surfaces were studied with Hall current and constant magnetic field. It is so complicated to similarity transform from curvilinear form of governing equations. Considering the similarity functions and variable, simultaneous governing equations in curvilinear coordinates is transformed to simultaneous nonlinear ODEs. The boundary conditions are converted into initial conditions by shooting method and solving the simultaneous ordinary differential equations numerically by RK-6 integration scheme. As for the results of computations, the following conclusions/achievements are made:

i. For nonlinear Casson parameter we have considered $A = \pm 0.5$. For several values of Casson parameter λ, $u-$ and $v-$ velocities are decelerating with accelerating values of λ in certain domain for $A = 0.5$ after that opposite results are found for $A = -0.5$. That is primary and secondary both boundary layer separations are found for large domain similarity variable ϕ.

ii. For large value of primary buoyancy force $\frac{U_F^2}{U_e^2} = 50$, the primary momentum thickness and energy thickness were reduced for increasing P_w.

iii. Momentum and energy thickness are reduced for the increasing P_w with large buoyancy force $\frac{V_F^2}{V_e^2} = 50$.

iv. It is found that increasing suction parameter P_w leads both skin frictions (primary and secondary) increase, and the heat flux reduces.

v. The absorption is to make contraction both momentum and energy layers thickness. Therefore, both velocity $(f_\emptyset, g_\emptyset)$ profiles as well as temperature profiles $(\vartheta_\emptyset)$ decrease with heat absorption $(\beta < 0)$ decreasing. Reverse actions are gotten for generation $(\beta > 0)$. Energy layer thickness increases with heat generation increases. It is also found the heat generation is to augment the momentum and energy profiles.

vi. Heat generation and absorption are fundamental concepts in thermal engineering. Heat absorption refers to the process where a material takes heat from its surroundings, often leading to an increase in temperature. Generation of heat can occur through various processes such as chemical reactions, electrical resistance, or friction.

vii. Application of a magnetic force is orthogonal with flow direction, that is, the drug strength like the Lorentz strength that tends to oppose flow and thus reduce its velocity. Hall current (Ω) plays the same role of dimensionless magnetic field (M) on the momentum.

Acknowledgement:

All authors gratefully acknowledge the American International University-Bangladesh for providing comprehensive logistical support in conducting this research. Also, thanks in advance for providing the suitable financial remuneration after confirmation (Published) of publication.

Future Work: Following research paper will be made in future:

Comparative investigation on $\gamma\, Al_2O_3 - H_2O$ and $\gamma\, Al_2O_3 - C_2H_6O_2$ Nanofluid Convective Flow Over Curvilinear Surfaces with Uniform Magnetic Field, Hall Current and Electric field and Slipping conditions.

Table1.

Effects of Heat absorption/generation (β) on the skin friction and Nusselt number for $m = n = c = 0.5$, $\frac{U_F^2}{U_e^2} = 10$, $\frac{V_F^2}{V_e^2} = 5$, $P_w = 0.5$, $P_r = 1.0$, $A = 0$, $M = \Omega = 0.5$

β	$f_{\emptyset\emptyset}(0)$	$g_{\emptyset\emptyset}(0)$	$\vartheta_\emptyset(0)$
-10	3.9047441	2.9379084	-3.5887762
-5	4.3599439	3.1165469	-2.7612213
-1	5.1011857	3.3908455	-1.7759055
0	5.4284229	3.5073781	-1.4191171
1	5.8843798	3.6644079	-0.9634403
5	5.4326820	3.8447402	0.3466725
10	6.4542249	4.2838730	3.2508244

Table 2.

Effects of injection/suction (P_w) on the skin friction and Nusselt number for $m = n = c = 0.5$, $\frac{U_F^2}{U_e^2} = 10$, $\frac{V_F^2}{V_e^2} = 5$, $\beta = 0.5$, $P_r = 1.0$, $A = 0$, $M = \Omega = 0.5$

P_w	$f_{\emptyset\emptyset}(0)$	$g_{\emptyset\emptyset}(0)$	$\vartheta_\emptyset(0)$
-1.50	3.8584707	1.8588956	0.3406179
-1.00	4.7447543	2.2418203	0.3133610
-0.50	5.3794662	2.6682845	0.0526940
0.00	5.6306104	3.1178412	-0.4729935
0.50	5.6336460	3.5797204	-1.2081324
1.00	5.6542947	4.0721959	-2.0607795
1.50	5.8417005	4.6301254	-2.9628525

Table 3.

Comparison between the numerical results of Falkner-Skan equation by Vasile Marinca [47] and the present work for $\frac{2m}{m+1} = 0.5$, and all other parameters are considered zero.

	Present work	Vasile Marinca et al. [47]	
ϕ	$f'(\phi)$	$f'(\phi)$	Relative error
0.8	0.5833040535	0.5833048176	1.30995E-06
2.4	0.9761011356	0.9760687525	3.3176E-05
4.0	0.9998096161	0.9998081985	1.41787E-06
5.6	0.9999998432	0.9999998399	3.3E-09
7.2	1.0000000000	0.9999999998	5E-10

References

[1] A. G. Hansen, "Possible similarity solution of the laminar incompressible boundary layer equations," ASME paper 57 A, pp79, 1957.

[2] Md. Zakerullah, and Kh. A. Maleque, "Similarity requirements for combined forced and free convective laminar boundary layer flow over vertical curvilinear surfaces," J. Bangladesh academy of sciences, Vol-22(1), pp 79, 1998.:

[3] KA Maleque, "Similarity Requirements for Mixed Convective Boundary Layer Flow over Vertical Curvilinear Porous Surfaces with Heat Generation/Absorption", *International Journal of Aerospace Engineering*, vol. 2020, Article ID 7486971, 9 pages, 2020. https://doi.org/10.1155/2020/7486971.

[4] T. Cebeci, K. Kaups, and A. Moser, "Calculation of three-dimensional boundary Layer," AIAA journal 14(8), pp. 1090, 1976.

[5] A. F. Blumberg, and H. J. Herring, " Circulation modelling using orthogonal curvilinear coordinates," In Elsevier oceanography series, vol-45, pp. 55, 1987.

[6] T. K. Hung, and T.D. Brown, "An implicit finite-difference method for solving the Navier-stokes equation using orthogonal curvilinear coordinates," Journal of Computational Physics, Vol 23(4), pp. 343, 1977.

[7] Redzic, V. Dragan, "The operation ∇ in orthogonal curvilinear coordinates", European Journal of Physics, vol 22(6), pp. 595, 2001.

[8] Mario Krzyk, and Matjaz Cetina, "Analysis of flow in a curved channel using the curvilinear orthogonal numerical mesh,"Journal of Mechanical Engineering, DOI:105545/sv-jme.2017.5183, Corpus ID:201799831, 2019.

[9] A. Shafiq, S. Nadeem, and Nurmuhammad, "Boundary layer flow over a curve surface imbedded in porous medium," Communications in theoretical physics, Vol-71, pp-344, 2019,

[10] Kianoosh, Youseki and Fabrice Veron, "Boundary layer formulations in orthogonal curvilinear coordinates for flow over wind generated surface waves," Journal of Fluid Mechanics, Vol-888, A11, 2020.

[11] E. Barakhovskaia, A. Glushchuk, P. Queeckers, and S. I. Carlo, "Stabilisation of condensate flow from curvilinear surfaces by means of porous media for space applications," Experimental thermal and fluid science, vol-121, 1 February, 2021, 110283.

[12] A. Meneghetti, B.E.J. Bodmann, and M.T.M.B, Vilhena, "On viscous fluid flow in curvilinear coordinate system," Integral methods in science and engineering (conference paper), 22 May. 2022.

[13] KA Maleque, "Combined fluid and ferrofluid buoyancy force, heat absorption and nonlinear ferro-viscosity effects on ferro-hydrodynamics fluid flow in orthogonal porous surface. Latin American Applied Research (LAAR), 54 (4), pp. 56, 2024.

[14] KA Maleque,, and MA Sattar, "Transient convective flow due to a rotating disc with magnetic field and heat absorption effects." Journal of energy, heat, and mass transfer. Vol-25, pp-279, 2003.

[15] KA Maleque, "Effects of Binary Chemical Reaction and Activation Energy on MHD Boundary Layer Heat and Mass Transfer Flow with Viscous Dissipation and Heat Generation/Absorption." International Scholarly Research Notices, Hindawi Publishing Corporation ISRN Thermodynamics Volume 2013, Article ID 284637, 9 pages, 2013. http://dx.doi.org/10.1155/2013/284637.

[16] Kh A Maleque (2014): A Binary Chemical Reaction on Unsteady Free Convective Boundary Layer Heat and Mass Transfer Flow with Arrhenius Activation Energy and Heat Generation/Absorption," The Latin American Applied Research Journal (LAAR), Argentina, Vol -44(1) pp- 97, 2014. ISSN: 0327-0793,
DOI: https://doi.org/10.52292/j.laar.2014.425.

[17] KA Maleque, "Numerical solution of combined forced and free convective flow in porous curvilinear surfaces in presence of heat absorption/generation, Latin American Applied Research (LAAR)-An international journal 55 (1), pp. 95, 2025.

[18] MK Abdul, "The thermal absorption/generation on ferro-fluid combined convective flow over curvilinear porous surfaces," AIUB journal of science and engineering (AJSE), vol 22, No. 3, pp 223, December, 2023. DOI: https://doi.org/10.53799/ajse.v22i3.546

[19] K. Ramesh, S. Jagadha, D. Gopal, S. H.S. Naik, and N. Kishan, " One Dimensional Radiative Nanofluid Flow with Heat Generative Al2 O3-H2O and Cu-H2O Nanoparticles Reactions Chemically," AIP Conf. Proc. 2943, December 2023; https://doi.org/10.1063/5.0190329.

[20] P. Jalili, S. Mousavi, B. Jalili, P. Pasha, and D. D. Ganji (2024): Thermal evaluation of MHD Jeffrey fluid flow in the presence of heat source and chemical reaction," International journal of modern physics, vol. 38, No. 08, 2024, 450113,https://doi.org/10.1142/S0217979224501133

[21] RK. Dash, KN Metha, and G. Jayaraman, " Casson fluid flow in a pipe filled with a homogenous porous medium, Int J Eng Sci; 34(10):1145-1156, 1996.

[22] Swati Mukhopadhyay, Prativa Ranjan De, Krishnendu Bhattacharyya, G.C. Layek, "Casson fluid flow over an unsteady stretching surface. Ain Shams Engineering Journal (Engineering Physics and Mathematics), 2013, 4, pp-933, 2013

[23] S. Nadeem , Rizwan UI Haq, Noreen Sher Akbar, Z. H. Khan, " MHD three-dimensional Casson fluid flow past a porous linearly stretching sheet." Alexandria Engineering Journal, 2013, 52, 577-582, 2013

[24] H. Kataria, Patel HR, "Radiation and chemical reaction effects on MHD Casson fluid flow past an oscillating vertical plate embedded in porous medium." Alexandria Engineering Journal, Vol. 55, issue 1, pp-583, March, 2016.

[25] Kh .A. Maleque, "MHD Non-Newtonian Casson fluid heat and mass transfer flow with exothermic/endothermic binary chemical reaction and activation energy," American Journal of Heat and Mass Transfer, vol.3, pp. 166, 2016.

[26] Kh. A. Maleque, "Unsteady MHD Non-Newtonian Casson Fluid Flow due to a Porous Rotating Disk with Uniform Electric Field." Fluid Mech Open Acc, vol. 3: pp-123, 2016a. doi:10.4172/fmoa.1000123

[27] Kh. A. Maleque, "Effect of Hall Current on MHD Non-Newtonian Unsteady Casson Fluid Porous Rotating Disk Flow with a Uniform Electric Field," The Aiub Journal of Science and Engineering, vol. 16 (02), pp-51, 2017.
DOI: https://doi.org/10.53799/ajse.v16i2.79

[28] T. Anwar, P. Kumam, and W. Watthayu, "Unsteady MHD natural convection flow of Casson fluid incorporating thermal radiative flux and heat injection/suction mechanism under variable wall conditions," *Sci Rep* **11**, pp-4275, 2021. https://doi.org/10.1038/s41598-021-83691-2.

[29] S.S. Reddy, K. Govardhan K, G. Narender, and S. Mistra, "3D radiation flow of unsteady Casson fluid with viscous dissipation effect," Iraqi Journal of Science, vol-64, No. 8, pp 4018, 2023. DOI:1024996/ijs.2023.64.8.26

[30] L.A. Lund, A. Asghar, G. Rasool, and U. Yashkun, "Magnetized casson SA-hybrid nanofluid flow over a permeable moving surface with thermal radiation and Joule heating effect," Case Studies in Thermal Engineering, Vol 50, 103510, October, 2023. https://doi.org/10.1016/j.csite.2023.103510.

[31] P. Jalili, A. A. Azar, B. Jalili, D.D. Ganji, "Study of nonlinear radiative heat transfer with magnetic field for non-Newtonian Casson fluid flow in a porous medium," Results of Physics, vol 48, 106137, 2023. https://doi.org/10.1016/j.rinp.2023.106371.

[32] Pop, I., "The effect of Hall currents on hydromagnetic flow near an accelerated plate". (English) Zbl 0229.76074, **J. Math. Phys. Sci., Madras 5, pp. 375**, 1971

[33] Gupta, A.S, "Hydromagnetic flow past a porous flat plate with hall effects. *Acta Mechanica* **22**, pp. 281, 1975. https://doi.org/10.1007/BF01170681

[34] Nanigopal Datta, and Rabindra Nath Jana, "**Oscillatory Magnetohydrodynamic Flow past a Flat Plate with Hall Effects, J. Phys. Soc. Jpn. 40, pp. 1469-1474,** 1976. **https://doi.org/10.1143/JPSJ.40.1469**

[35] Ram, P. C., "Hall Effects on the Hydromagnetic Free Convective Flow and Mass Transfer Through a Porous Medium Bounded by an Infinite Vertical Porous Plate with Constant Heat Flux". International journal of energy research, 12, 227, 1988. **https://doi.org/10.1002/er.4440120205**

[36] Sattar, Md. A., "Unsteady hydromagnetic free convection flow with hall current mass transfer and variable suction through a porous medium near an infinite vertical porous plate with constant heat flux". International journal of energy research, 18(9), pp-771, 1994. **https://doi.org/10.1002/er.4440180902**

[37] Ahmed L. Aboul-Hassan, Hazem Ali Attia, "Flow due to a rotating disk with Hall effect" Physics Letters **A 228**, pp. 286, 1997. https://doi.org/10.1016/S0375-9601(97)00086-8

[38] KA Maleque, MA Sattar, "The effects of variable properties and Hall current on steady MHD laminar convective fluid flow due to a porous rotating disk", International Journal of Heat and Mass Transfer 48 (Nov.), 4963-4972,, 2005 ISSN: 0017-9310.

[39] KA Maleque, "Effects of combined temperature-and depth-dependent viscosity and Hall current on an unsteady MHD laminar convective flow due to a rotating disk". Chemical Engineering Communications(Taylor and Francis), 197(4), 506-521, 2009. **ISSN** 0098-6445.

[40] Z. Uddina, and M. Kumarc, "Hall and ion-slip effect on MHD boundary layer flow of a micro polar fluid past a wedge, Scientia Iranica B . 20 (3), pp. 467, 2013.

[41] D. Srinivasacharya and Md. Shafeeurrahman, " Hall and ion slip effects on mixed convection flow of nanofluid between two concentric cylinders, Journal of the Association of Arab Universities for Basic and Applied Sciences, vol 24, pp. 223, 2017.

[42] Veera Krishna M, "Hall and ion-slip effects on MHD free convective rotating flow bounded by the semi-infinite vertical porous surface". *Heat Transfer* ,2020; 49(4): 1920–1938, 2020. **https://doi.org/10.1002/htj.21700**

[43] Jitendra Kumar Singh, Suneetha Kolasani, and Gauri Shenker Seth, "Scrutiny of induced magnetic field and Hall current impacts on transient hydromagnetic nanofluid flow within two vertical alternative magnetized surfaces". Proceedings of the Institution of Mechanical Engineers, Part E: Journal of Process Mechanical Engineering, Vol 237 (4), pp.1595, 2023. https://doi.org/10.1177/09544089221119255

[44] P. R. Nachtsheim, and P. Swigert,"Satisfaction of asymptotic boundary conditions in numerical solution of system of nonlinear of boundary layer type," NASA TN-D3004, 1965.

[45] H. Schlichting, "Boundary layer theory,", McGraw-Hill Book Company, New York, Sixth Edition pp-151, 1968.

[46] E. M. Sparrow, R. Eichorn, and L. J. Gregg, "Combined forced and free convection in a boundary layer flow," Phys. Fluids, Vol-2, pp-319, 1959.

[47] Vasile Marinca, R. Daniel Ene, and B. Marinca, "Analytical approximate solution for Falkner-Skan equation," The scientific world Journal (Hindawi publishing corporation), Volume 2014, Article ID: 617453, 2014. https://doi.org/10.1155/2014/617453

DR. KH. ABDUL MALEQUE was born in Tangail, Bangladesh, in 1966. He received the M. Sc. degree in Applied Mathematics from Dhaka University, Bangladesh, the M. Phil. degree in Applied Mathematics from Bangladesh University of Engineering and Technology (BUET) and the Ph. D. degree in Applied Mathematics from Dhaka University, Bangladesh. He joined as a faculty member in the Department of Mathematics, American International University-Bangladesh, Dhaka, Bangladesh (AIUB) in 1996. At present, he is teaching as a professor at AIUB. His field of research is Fluid Mechanics (Incompressible/Compressible flow, Flow due to rotating disk, boundary layer flow in orthogonal curvilinear surfaces, MHD flow, Polar fluid flow, Convective flow etc). He has 43 foreign and local publications in the various fields of Fluid Mechanics. He is a reviewer of the following renowned Journals: International Journal of Heat and Mass Transfer; Chemical Engineering Communications USA; Latin American Applied Research (An International Journal, Heat and Mass Transfer division) Argentina; The AIUB Journal of Science and Engineering, Bangladesh; Bangladesh Journal of Scientific and Industrial Research, Bangladesh; The Journal of Lithuanian Association of Nonlinear Analysts (LANA); Indian Journal of Mathematics (IJM)/Bulletin of the Allahabad Mathematical Society (BAMS). He is the life member of Bangladesh Mathematical Society and Alumni of Mathematics Department, Dhaka University, Bangladesh.

KH SABIKUM MALEK was born in Dhaka, Bangladesh in 2000. She is the student at American International University-Bangladesh (AIUB) in the department of Electrical and Electronics Engineering